
# Modelling discomfort: How do drivers feel when cyclists cross their path?

Accident Analysis and Prevention 146 (2020) 105550

Contents lists available at ScienceDirect

Accident Analysis and Prevention

journal homepage: www.elsevier.com/locate/aap

# Modelling discomfort: How do drivers feel when cyclists cross their path?

Christian-Nils Boda[a,*], Marco Dozza[a], Pablo Puente Guillen[b], Prateek Thalya[a,c], Leila Jaber[d], Nils Lubbe[d]

[a] Chalmers University of Technology, Hörselgången 4, 417 56, Göteborg, Sweden
[b] Safety Research and Technical Affairs, Toyota Motor Europe, Zaventem, Belgium
[c] Veoneer Sweden AB, Wallentinsvägen 22, 447 37, Vårgårda, Sweden
[d] Autoliv Research, Wallentinsvägen 22, 44783, Vårgårda, Sweden

ARTICLE INFO

*Keywords:*
Driver behavior model
Driving simulator
Test track
Comfort
Active safety systems
Acceptability

ABSTRACT

Many cyclist fatalities occur on roads when crossing a vehicle path. Active safety systems address these interactions. However, the driver behaviour models that these systems use may not be optimal in terms of driver acceptance. Incorporating explicit estimates of driver discomfort might improve acceptance. This study quantified the degree of discomfort experienced by drivers when cyclists crossed their travel path. Participants were instructed to drive through an intersection in a fixed-base simulator or on a test track, following the same experimental protocol. During the experiments, three variables were controlled: 1) the car speed (30, 50 km/h), 2) the bicycle speed (10, 20 km/h), and 3) the bicycle-car encroachment sequence (bicycle clears the intersection first, potential 50 %-overlap crash, and car clears the intersection first). For each trial, a covariate, the car's time-to-arrival at the intersection when the bicycle appears ($TTA_{vis}$), was calculated. After each trial, the participants were asked to report their experienced discomfort on a 7-point Likert scale ranging from no discomfort (1) to maximum discomfort (7). The effect of the three controlled variables and the effect of $TTA_{vis}$ on drivers' discomfort were estimated using cumulative link mixed models (CLMM). Across both experimental environments, the controlled variables were shown to significantly influence discomfort. $TTA_{vis}$ was shown to have a significant effect on discomfort as well; the closer to zero $TTA_{vis}$ was (i.e., the more critical the situation), the more likely the driver reported great discomfort. The prediction accuracies of the CLMM with all three controlled variables and the CLMM with $TTA_{vis}$ were similar, with an average accuracy between 40 and 50 % for the exact discomfort level and between 80 and 85 % allowing deviations by one step. Our model quantifies driver discomfort. Such model may be included in the decision-making algorithms of active safety systems to improve driver acceptance. In fact, by tuning system activation times depending on the expected level of discomfort that a driver would experience in such situation, a system is not likely to annoy a driver.

## 1. Introduction

For more than two decades, many countries have made great efforts to encourage their populations to switch from driving cars to public transportation or cycling (Martens, 2007; Pucher et al., 2011; Börjesson and Eliasson, 2012; Scheepers et al., 2014). Cycling is a healthy activity with benefits in terms of cost, travel time, and the environment. However, the activity is not without risk, as the accident statistics show (European Commission, 2017). In the European Union, the generally decreasing trend of driver fatalities (European Commission, 2017) is not matched by the trend of cyclist fatalities, which has levelled off in recent years (European Commission, 2017). Cyclist fatalities in vehicle-bicycle crashes at unsignalised intersections account for a significant part of all cyclist fatalities (Schepers et al., 2011, 2016). Additionally, in a systematic review, Prati et al. identified many studies pointing out that vehicle-bicycle crashes were more likely to happen at an unsignalised intersection (Prati et al., 2017).

Improvements in road infrastructure together with new active safety systems—such as autonomous emergency braking systems (AEB) and forward-collision warning systems (FCW)—and automated driving systems could help to reduce the number of cyclist fatalities in the vehicle-bicycle intersection scenario. Nowadays, some active safety systems integrate functions to detect and avoid collisions with vulnerable road users such as pedestrians (Tsuchida et al., 2007; Hayashi et al., 2013) and cyclists (Ljung Aust et al., 2015). These systems are included in car safety performance assessment protocols. For example,

* Corresponding author.
*E-mail address:* christian-nils.boda@chalmers.se (C.-N. Boda).

https://doi.org/10.1016/j.aap.2020.105550
Received 15 February 2019; Received in revised form 21 October 2019; Accepted 10 April 2020
Available online 15 September 2020

Euro NCAP (European new car assessment programme) assesses the safety performances of AEB —but not FCW— in bicycle-crossing scenario since 2018 (Euro NCAP, 2018). However, active safety systems designed to improve vulnerable road users' safety are not able to avoid all crashes yet. The sensors' capabilities have been improving continuously over the last few years, improving the detection of vulnerable road users, but still lack a complete driver model which manages to avoid unappreciated activations and thereby annoying drivers without compromising effectiveness in avoiding collisions. Driver behaviour in interactions with cyclists at unsignalised intersections has been scarcely studied, and very few driver models that predict driver behaviour are available in the literature (Silvano et al., 2016).

The benefits of active safety systems and automated driving systems strongly depend on driver acceptance (Adell et al., 2014). They should, therefore, be designed to improve driver acceptance while fulfilling their purpose of assisting the driver or controlling the vehicle. Adell et al. (2014) defined driver acceptance as "the degree to which an individual incorporates the system in his/her driving". Informed by the work of Ljung Aust and Engström (2010) and Summala (2007); Lubbe and Rosén (2014) suggested that active safety system activation is only relevant when drivers are no longer in their comfort zone—that is, they feel discomfort. This idea can be extended to automated driving systems as well: drivers may be more likely to accept an automated driving system if it stays within the drivers' comfort zone. In this paper, the definition of discomfort is derived from Summala (2007) who theorized that discomfort can be assimilated to the concept of risk in the zero-risk theory; speculating that drivers control their vehicle to reduce their feeling of discomfort (Engström, 2011). Systems such as FCW based on measurable metrics (including drivers' reaction time (Jamson et al., 2008), time-to-contact (Dagan et al., 2004), or required deceleration for avoiding a crash (Kiefer, 2000)) do not explicitly consider how drivers perceive the criticality of an event that would require a system intervention. It is discussed in the literature that driver acceptance of safety systems would be improved if the systems would be able to partly base their interventions on the perceived criticality of the event (Brännström et al., 2013; Ljung Aust and Dombrovskis, 2013; Ljung Aust et al., 2015). The sense of criticality of a driving event is part of driver discomfort (Summala, 2007). It is, therefore, hypothesized that the integration of a discomfort estimation algorithm in the systems' decision algorithm would increase driver acceptance by making sure that the system intervenes in situations in which a (fit-to-drive, attentive) driver would experience discomfort. As a result, it is important to better understand how driver discomfort relates to external cues. A previous study of driver-cyclist interactions at unsignalised intersections showed that the brake-onset response was driven by a metric based on visual cues (Boda et al., 2018): the closer in time the vehicle was to the intersection when the bicycle appeared, the faster drivers braked. The car's time-to-arrival to the intersection —a continuous metric—(TTA) was computed, and the value of TTA at the moment when the bicycle starts to be visible ($TTA_{vis}$) was used in the analyses. The results of Boda et al. (2018) could be explained by Markkula et al. (2016)'s accumulation model, which states that the more salient a cue is, the faster the accumulation of cues, and hence the reaction (i.e. braking or steering), will be. The saliency (i.e. criticality) of a cue was suggested to be directly related to the feeling of discomfort. Therefore, one of the hypotheses of the present study is that the shorter $TTA_{vis}$, the greater the driver's discomfort. Due to the study design, the variable $TTA_{vis}$ was a covariate of the independent variables (i.e., car speed, bicycle speed, and bicycle-car encroachment sequence).

The objectives were: 1) to quantify the effect of car speed, bicycle speed, and bicycle-car encroachment sequence on discomfort; 2) to quantify the effect of $TTA_{vis}$ on discomfort; 3) to propose a model which predicts the level of discomfort and can therefore inform the designs of active safety systems and automated driving systems, and improve Euro NCAP protocols.

## 2. Methodology

Both simulator and the test-track experiments were conducted following the same protocol, to evaluate driver interaction with a cyclist in a crossing scenario. The former was carried out in a fixed-base simulator at SAFER, Gothenburg (Sweden) while the latter was carried out at Autoliv, in Vårgårda (Sweden). Information about the discomfort experienced by the participants was collected with questionnaires. Before carrying out the experiments, an ethical approval application was sent to the ethical review board of Gothenburg (*Etikprövningsnämnden*, Dnr 146-16). The ethical review board did not raise any ethical concerns about the study.

### 2.1. Participants

Ninety-one participants, who were older than 25 years and had a valid driver license, participated in the study: 47 in the simulator experiment and 44 in the test-track experiment. In the simulator experiment, the participants were recruited through advertising flyers in public places (i.e. supermarkets and parking lots) and through a mailing list. In the test-track experiment, the participants were recruited through an internal mailing list at Autoliv, Vårgårda. The data collected for nine participants in the simulator experiment, and one participant in the test-track experiment, were excluded from the analyses because these participants felt motion sick or failed to follow the instructions. The participants in the simulator experiment had an average age of 40.6 years (standard deviation; SD = 13.1), and 37.0 % were female. Similarly, the average age of the participants in the test-track experiment was 41.9 years (SD = 10.8), 32.6 % of them were female. Participants in the simulator experiment drove an average yearly mileage of 11,500 km (median = 10,000 km, range = [300, 45,000] km), and participants in the test-track experiment drove an average yearly mileage of 18,000 km (median = 20,000 km, range = [1000, 35,000] km). Before their participation, each volunteer had to sign a consent form which explained the reason of the study, the potential risks, and the participants rights; for instance, participants were informed that they could stop the experiment at any time without giving any justification.

### 2.2. Study setup

#### 2.2.1. Scenario layout

In both experiments, participants started to drive through an intersection from a distance of 180 m and interacted with a bicyclist entering the intersection from the right side (Fig. 1). A stationary car was placed 30 m away from the intersection in the opposite lane to simulate oncoming traffic. Participants were instructed to drive and behave as they would in normal traffic, and a speed limiter was used to ensure that the instructed speed was respected.

#### 2.2.2. Independent variables

For each trial, the participants drove through the intersection with a velocity ($V_{car}$) of either 30 or 50 km/h, depending on the trial. They reached the instructed speed before interacting with the bicycle, which had a set speed ($V_{bicycle}$) of 10 or 20 km/h. Three bicycle-car encroachment sequences were used during the experiment: 1) the bicycle clears the intersection before the car, 2) the bicycle is in a 50 %-overlap with the car's front bumper, and 3) the car clears the intersection before the bicycle. The continuous variable $Lat_{arr}$ was used in the analyses to describe the bicycle-car encroachment sequence. $Lat_{arr}$ corresponds to the projected lateral distance between the bicycle and the car when the car reaches the intersection (negative values when the bike is at the left side of the car, positive values when located at the right).

#### 2.2.3. Test environments

The fixed-base simulator used in the simulator experiment

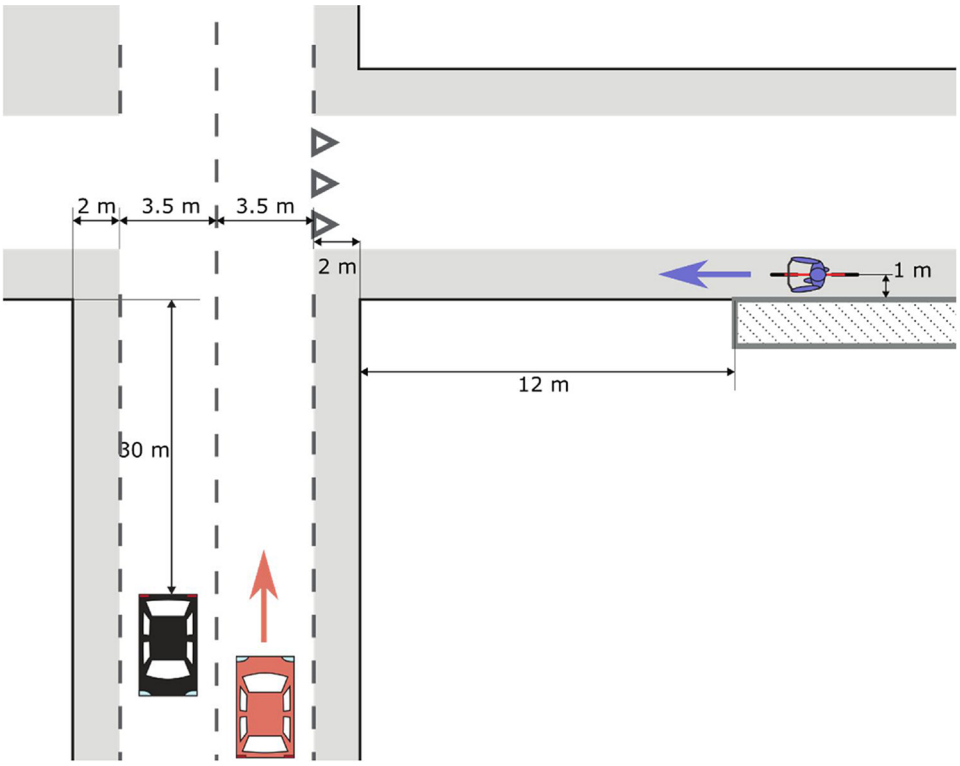


**Fig. 1.** Experiment layout: the stationary car is dark grey, the driven car is orange, and the bicycle robot is purple. Arrows show the direction of travel of the car driven by the participants and the bicycle robot (For interpretation of the references to colour in this figure legend, the reader is referred to the web version of this article).

comprised three screens covering about 150 degrees of the field of view, and a Logitech G27 steering wheel with pedals. The virtual environment was modelled as closely as possible to the environment of the test-track experiment. The cyclist model was created with MakeHuman and animated together with the bicycle model with Blender 3D. The whole simulation was generated by OpenDS, an open-source driving simulator software. (Detailed information on the experiments' setup can be found in Boda et al. (2018)). The data collected in both experiments included the car's position and speed and the gas and brake pedals' positions, as well as the position and speed of the bicycle.

#### 2.2.4. Experimental protocol

The experiments consisted of 20 trials, 12 trials corresponding to a full factorial design with two levels for $V_{bicycle}$, two levels for $V_{car}$, and three levels for bicycle-car encroachment sequence. For these 12 trials, four trials were added in which the bicycle braked before entering the intersection to minimize the participants' expectancy that the cyclist would always cross the road. Four empty—no bicycle crossing—trials were also added to reduce expectancy. In the simulator experiment, a surprise trial was added as the 21 st trial: a bicyclist appeared at the last moment when the drivers drove back through the intersection at the end of the experiment. In the simulator and test-track experiments, all participants started with a test drive that lasted about 5 min and finished with an empty trial. The order of all trials, apart from the empty trials (and the surprise trials in the simulator experiment), were randomized (Fig. 2).

Before starting the experiment, participants were informed that they will drive multiple times through the intersection at different speeds and that a cyclist could cross their path. They were asked to drive and behave as they would normally do on real roads.

After each trial, the participants reported their discomfort on a 7-point Likert scale from 1 (no discomfort) to 7 (maximum discomfort). This question was followed up by additional questions, to understand 1) whether drivers understood the discomfort scale and 2) what parameters played a role in the scoring. The additional questions were used in the present study to filter out the data in which the participants may have misunderstood the discomfort scale, or may have experienced discomfort from a source other than the actual driving scenario (e.g., stress due to being observed, motion sickness, etc.).

### 2.3. Data analyses

The trials derived from the full factorial design (12 per participant) were analysed. The SIM and TT datasets include these trials for all participants in the simulator and test-track experiments, respectively. An additional dataset, called SIMST, included the same trials as the SIM dataset and the surprise trial for all participants (i.e. 21st trial in Fig. 2). In this section, the cumulative link mixed models (CLMM) are introduced, followed by the description of the analyses of 1) the effect of the controlled variables (speeds and bicycle-car encroachment sequence) on discomfort, 2) the effect of $TTA_{vis}$ on discomfort, and 3) the prediction performances of the models.

#### 2.3.1. Cumulative link mixed models

The two CLMMs described in this paper explored the effect of different variables on discomfort: the first considered the three controlled variables, and the second considered $TTA_{vis}$. They are described in more detail below. The fit of CLMMs was done with the R-package "ordinal"

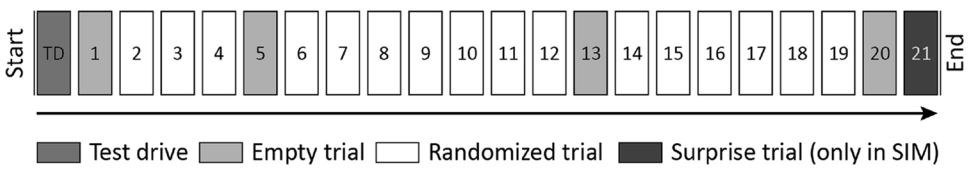


**Fig. 2.** Schematic representation of the order of trials in the experiments.

(Christensen, 2015). The CLMMs are an extension of the general linear mixed effect model, which analyses the effect of fixed and/or random effects on ordinal data, using *logit* as the link function (Agresti, 2013) (Eq. (1)).

$$logit[X] = log\left(\frac{X}{1-X}\right) \quad (1)$$

If $Y_{it}$ is the observation $t$ in cluster $i$ of the ordinal response, the corresponding CLMM can be written as in Eq. (2). Let $\beta$ denote a vector of fixed effects, $u_i$ a vector of random effects for cluster $i$, and $\theta_j$ a value, the *cut-point,* that represents the intercept dependent on the category $j$. Additionally, $x_{it}$ is a column vector of explanatory variables for the observation $t$ in cluster $i$, and $z_{it}$ is a column vector of scaling parameters of the random effects for the observation $t$ in cluster $i$. $J$ corresponds to the number of categories of the response variable (i.e., in the present study J = 7 corresponding to the seven levels of discomfort score). The variability of the random effects follows a normal distribution $N(0, \Sigma)$ centred on zero with variance Σ; CLMM estimates this variance for each random effect.

$$\text{logit}[P(Y_{it} \le j|u_i)] = \theta_j - x_{it}^T\beta - z_{it}^T u_i, j = 1, \ ...,J-1 \quad (2)$$

In this paper, the response (discomfort score) ranged from 1 to 7. The CLMMs were used to estimate the effect (i.e., **β**) of the variables of interest (i.e., $\mathbf{x}_{it}$) on the discomfort score. In the analysis presented in the next section, the random effect due to the subjects was estimated (i.e., $\mathbf{u}_i$) to account for the variability between participants. Since only one random effect was studied, the cluster $i$ corresponds to the set of observations related to the participant $i$ ($i$ taking the value from 1 to the number total of participants included in the analysis).

In the analysis, the odds ratios (OR), easily derivable from CLMMs, were used to interpret the results. The odds of observing lower scores can be calculated from the fixed effect's estimate as in Eq. (3) (see (Christensen, 2015). If the estimated OR is bigger than one, it means that the (fixed) effect increases the odds of having a lower score. If the predictor associated with the fixed effect of interest is continuous, the OR will be expressed by one unit of this predictor. Note that to estimate the OR when passing from the value $x_1$ to the value $x_2$ of a continuous predictor, the OR should be computed as in Eq. (4).

$$OR(\beta_i) = exp(-\beta_i) \quad (3)$$

$$OR((x_2 - x_1) \times \beta_i) = \exp((x_1 - x_2) \times \beta_i) \quad (4)$$

### 2.3.2. Effect of controlled variables on discomfort score

For each experiment, the effects on discomfort score of the speeds ($V_{bicycle}$ and $V_{car}$) and the car-bicycle encroachment sequence ($Lat_{arr}$) were estimated. The estimates were devised by fitting a CLMM including one random effect on the cut-points/intercept; *subject.* This variable corresponds to each individual in the experiment. Including this random effect means the study can estimate the variability between subjects. The formula describing this CLMM is shown in Eq. (5). This model, denoted CLMM($V_{bicycle}$, $V_{car}$, $Lat_{arr}$), was fitted to the SIM, SIMST, and TT datasets.

$$\text{logit}[P(discomfort_{it} \le j|u_{it})] = \theta_j - \begin{bmatrix} V_{bike} \\ V_{car} \\ Lat_{arr} \end{bmatrix}_{it}^T \beta - \text{subject}_i \quad , j = 1,...,6 \quad (5)$$

In this expression, $\beta$ is a 3-element vector that includes an estimate of each fixed effect.

### 2.3.3. Effect of $TTA_{vis}$ on discomfort score

The effect of the visual-cue-based variable, $TTA_{vis}$, on discomfort scores was analysed by fitting a CLMM, defined in Eq. (6). The random effect due to subject (the variability between participants) was included in the model. This model, denoted CLMM($TTA_{vis}$), was fitted to the datasets from SIM, SIMST, and TT.

$$\text{logit}[P(discomfort_{it} \le j|u_{it})] = \theta_j - \text{TTA}_{vis_{it}}\beta - subject_i \quad , j = 1,...,6 \quad (6)$$

In this expression, $\beta$ is a 1-element vector that includes an estimate of the sole fixed effect ($TTA_{vis}$).

### 2.3.4. Estimation of prediction accuracy of the cumulative link mixed model

The prediction accuracy of each CLMM was evaluated through cross-validation. This method is not straightforward for non-linear mixed effects models such as CLMM, compared to models with only fixed effects (Colby and Bair, 2013), so the following process was used to account for the random effect in each model. First, the sampling always included data from each of the participants. Let $n$ be the number of trials per participant; the fit was made using $k$ trials per participant, and the model was used to predict the remaining $n$-$k$ trials. The Monte Carlo method was applied to study the variability of the prediction accuracy estimation. The $k$ trials per participants used for fitting the models were randomly sampled without replacement; this was iterated 200 times for each $k$. To study the effect of the number of trials used for

**Table 1**
Example of a confusion matrix; $c_{ij}$ represents the number of occurrences of the pair *(i,j)* for predicted score *(i)* and observed score (*j*).

| Predicted discomfort score | | | | | | | |
|---|---|---|---|---|---|---|---|
| 1 | $c_{11}$ | $c_{12}$ | $c_{13}$ | $c_{14}$ | $c_{15}$ | $c_{16}$ | $c_{17}$ |
| 2 | $c_{21}$ | $c_{22}$ | $c_{23}$ | $c_{24}$ | $c_{25}$ | $c_{26}$ | $c_{27}$ |
| 3 | $c_{31}$ | $c_{32}$ | $c_{33}$ | $c_{34}$ | $c_{35}$ | $c_{36}$ | $c_{37}$ |
| 4 | $c_{41}$ | $c_{42}$ | $c_{43}$ | $c_{44}$ | $c_{45}$ | $c_{46}$ | $c_{47}$ |
| 5 | $c_{51}$ | $c_{52}$ | $c_{53}$ | $c_{54}$ | $c_{55}$ | $c_{56}$ | $c_{57}$ |
| 6 | $c_{61}$ | $c_{62}$ | $c_{63}$ | $c_{64}$ | $c_{65}$ | $c_{66}$ | $c_{67}$ |
| 7 | $c_{71}$ | $c_{72}$ | $c_{73}$ | $c_{74}$ | $c_{75}$ | $c_{76}$ | $c_{77}$ |
| | 1 | 2 | 3 | 4 | 5 | 6 | 7 |

Observed discomfort score

fitting the models, the value of $k$ ranged from two to 11 for the SIM and TT datasets, and from two to 12 for the SIMST dataset.

For each iteration for each $k$ value, a confusion matrix (Table 1) was produced. Hence, for each $k$ value, 200 confusion matrices were produced. The number of correct predictions (i.e., when the predicted score is equal to the observed score) will be shown on the diagonal of the confusion matrix (i.e. $c_{ii}$, where i = [1, …, 7]). For a given iteration $t$, the overall accuracy ($Acc$) of the model can thus be defined as the ratio of the sum of the elements on the diagonal over the sum of all the elements in the matrix (Story and Congalton, 1986); see Eq. (7). The value for Acc was calculated for each confusion matrix for each $k$-value step. The average values of Acc for each $k$ value, together with a one-standard-deviation corridor, were plotted for CLMM($TTA_{vis}$) for each dataset (i.e. SIM, SIMST, and TT).

$$Acc(t) = \frac{\sum_{i=1}^{7} c_{ii}(t)}{\sum_{j=1}^{7}\sum_{i=1}^{7} c_{ij}(t)} \tag{7}$$

Finally, the confusion matrices for each dataset at the last $k$-value (i.e. k = 11 for SIM and TT, and k = 12 for SIMST) were reported to illustrate the performances of the models at each observed score.

## 3. Results

### 3.1. Effect of controlled variables on discomfort score

The effect of speeds (i.e. $V_{bicycle}$ and $V_{car}$) and the bicycle-car encroachment sequence ($Lat_{arr}$) on the discomfort score rating was estimated using the CLMM described in Eq. (5). The observed discomfort scores per variable in each experiment are displayed in Fig. 3: the boxplots show the distributions of $Lat_{arr}$ for each level of discomfort. As the levels of $V_{bicycle}$ or $Lat_{arr}$ increased, the discomfort scores were likely to be higher. For higher car speed ($V_{car}$), the discomfort scores were only slightly higher. Finally, when the variable $Lat_{arr}$ was closer to zero and grew positive, the discomfort scores were higher. This may be explained by the fact that when $Lat_{arr}$ was closer to zero there was greater potential for a collision (the car is more likely to crash into the bicycle); additionally, when $Lat_{arr}$ was positive, there was potential for a different collision, since the car has already entered the intersection (i.e. the bicycle would collide with the car laterally).

In this analysis, the random effects induced by the variability between participants were included. Fig. 4 shows, for each experiment, the frequency of each observed discomfort score per participant. The variability between participants between the two experiments seems to be of similar magnitude.

The results of CLMM($V_{bicycle}$, $V_{car}$, $Lat_{arr}$) for SIM and TT are reported in Table 2, and in Table 3 for SIMST. The first observation is that all the estimates for SIM, SIMST, and TT were statistically significant ($p < 0.05$). Additionally, the estimates of the fixed and random effects are of similar size across experiments.

The OR results for the fixed-effects estimates suggest that the effects from $V_{bicycle}$ and $Lat_{arr}$, but not $V_{car}$, were substantial. The OR of having a higher discomfort score when increasing $V_{bicycle}$ by 1 km/h was 1.23 for SIM, 1.22 for SIMST, and 1.28 for TT. Similarly, the OR of having a higher discomfort score when increasing $Lat_{arr}$ by 1 m was 1.36 for SIM, 1.15 for SIMST, and 1.32 for TT. For $V_{car}$, the odds ratio was 1.02 for

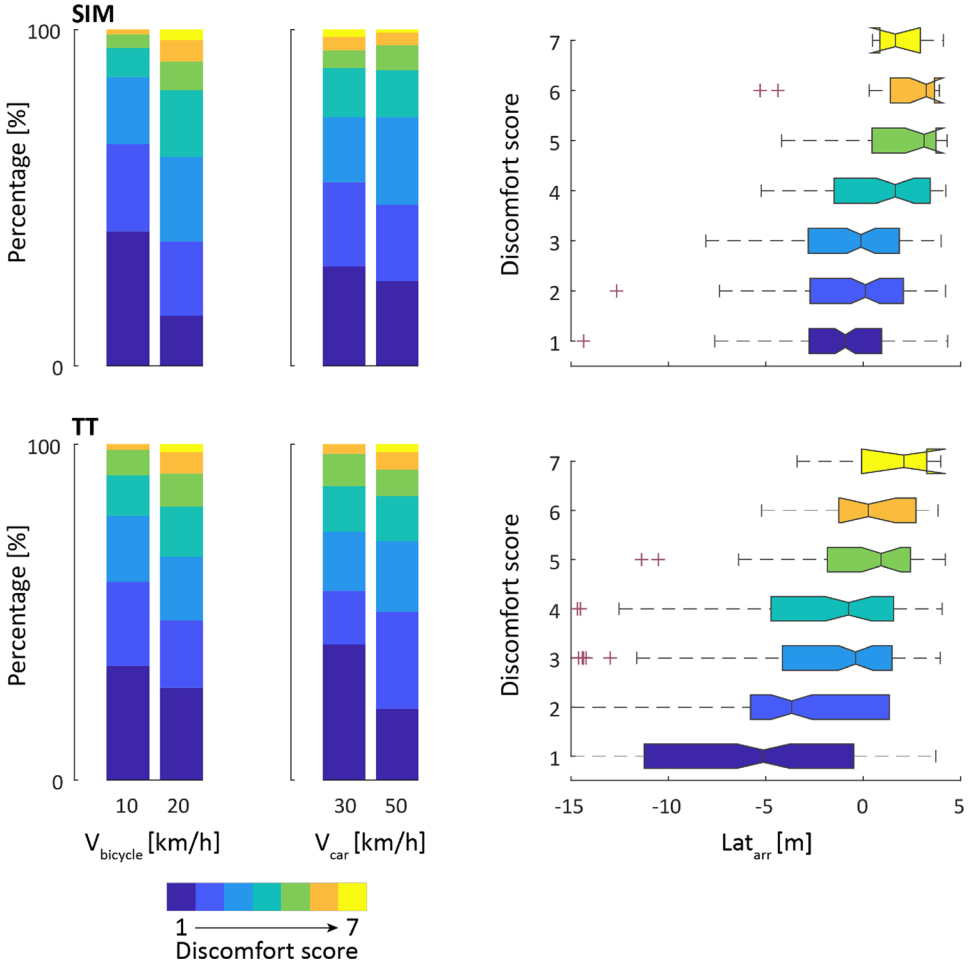


**Fig. 3.** Distributions of discomfort scores for the controlled variables ($V_{bicycle}$, $V_{car}$, and $Lat_{arr}$). Stacked histograms were used for the grouped variables $V_{bicycle}$ and $V_{car}$, and horizontal boxplots were used for the continuous variable $Lat_{arr}$.

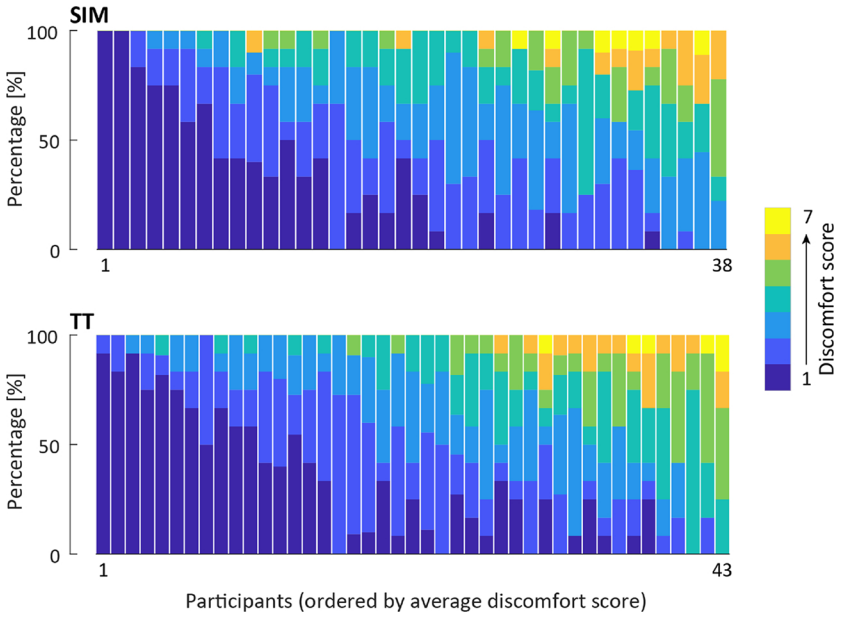


**Fig. 4.** Discomfort scores per participant ordered by participants' average score.

**Table 2**
Cumulative link mixed models for the simulator (excluding the surprise trial) and the test track.

| | | Simulator | | | Test track | | |
|---|---|---|---|---|---|---|---|
| Variables | | Estimate | SD | p-value | Estimate | SD | p-value |
| *Cut-points* | $\theta_1$ | 2.586 | 0.625 | | 2.329 | 0.596 | |
| | $\theta_2$ | 4.618 | 0.656 | | 4.197 | 0.616 | |
| | $\theta_3$ | 6.326 | 0.687 | | 5.840 | 0.639 | |
| | $\theta_4$ | 7.852 | 0.722 | | 7.419 | 0.674 | |
| | $\theta_5$ | 9.074 | 0.764 | | 9.097 | 0.730 | |
| | $\theta_6$ | 10.642 | 0.851 | | 11.047 | 0.857 | |
| *Fixed effects* | $\beta(V_{bicycle})$ | 0.204* | 0.019 | < 0.001 | 0.249* | 0.023 | < 0.001 |
| | $\beta(V_{car})$ | 0.023* | 0.010 | 0.0177 | 0.023* | 0.010 | 0.0199 |
| | $\beta(Lat_{arr})$ | 0.303* | 0.035 | < 0.001 | 0.279* | 0.023 | < 0.001 |
| *Random effects* | subject | 4.645 | 2.155 | | 4.405 | 2.099 | |

*Note:* For random effects, *Estimate* corresponds to the estimate of the random effect variance. The star (*) represents the fixed effects that were statistically significant ($p < 0.05$). SD stands for standard deviation.

**Table 3**
Cumulative link mixed model for the simulator (including the surprise trial).

| Variables | | Estimate | SD | p-value |
|---|---|---|---|---|
| *Cut-points* | $\theta_1$ | 2.795 | 0.581 | |
| | $\theta_2$ | 4.556 | 0.609 | |
| | $\theta_3$ | 5.994 | 0.635 | |
| | $\theta_4$ | 7.170 | 0.658 | |
| | $\theta_5$ | 8.202 | 0.686 | |
| | $\theta_6$ | 9.359 | 0.727 | |
| *Fixed effects* | $\beta(V_{bicycle})$ | 0.197* | 0.018 | < 0.001 |
| | $\beta(V_{car})$ | 0.029* | 0.009 | 0.002 |
| | $\beta(Lat_{arr})$ | 0.138* | 0.026 | < 0.001 |
| *Random effects* | subject | 3.201 | 1.789 | |

*Note:* For the random effects, E(var.) is the estimate of the variance and E(std.) the estimate of its corresponding standard deviation. The star (*) represents the effects that were statistically significant ($p < 0.05$).

SIM, 1.03 for SIMST, and 1.02 for TT when increasing $V_{car}$ by 1 km/h.

Additionally, the variance due to the participant (shown by the random effect) supports what is seen in Fig. 4—that the variability between participants in each experiment, though large, was comparable between SIM and TT. However, the variability between participants for SIMST was smaller than for SIM or TT, which may be due to the fact that in the surprise trials the participants met their physical limits when reacting to a threat.

### 3.2. Effect of $TTA_{vis}$ on discomfort score

The effect of $TTA_{vis}$, $\beta(TTA_{vis})$, was estimated using CLMM($TTA_{vis}$) as described in Eq. (6), including the random effect due to the variability between participants. The results of the CLMM fits are summarized in Table 4 for SIM and TT, and in Table 5 for SIMST. The order of magnitude of each estimate of the cut-points, fixed effects, and random effects is similar across the three fits.

The estimates for $\beta(TTA_{vis})$ are -0.8696, -0.9537, and -0.7376 for SIM, SIMST, and TT, respectively. When the variable $TTA_{vis}$ decreases by one unit, the OR of having a higher discomfort score is 2.1 for SIM, 2.6 for SIMST, and 2.4 for TT.

The estimated variability between participants for each dataset is about 4.8 for SIM, 4.2 for SIMST, and 4.0 for TT. These three estimates are similar, suggesting again that the variability between the participants in the SIM and TT experiments are comparable.

Fig. 5 represents the observed discomfort score per participant for each dataset on the left-hand side; the right-hand side graphically illustrates the three fitted CLMMs for SIM, SIMST, and TT (see Tables 4 and 5). The graphs show the discomfort score versus a normally-

**Table 4**
Cumulative link mixed models for the simulator (excluding the surprise trial) and the test track.

| | | Simulator | | | Test track | | |
|---|---|---|---|---|---|---|---|
| Variables | | Estimate | SD | p-value | Estimate | SD | p-value |
| *Cut-points* | $\theta_1$ | −5.898 | 0.548 | | −5.848 | 0.521 | |
| | $\theta_2$ | −3.813 | 0.494 | | −4.112 | 0.487 | |
| | $\theta_3$ | −2.058 | 0.462 | | −2.572 | 0.465 | |
| | $\theta_4$ | −0.547 | 0.452 | | −1.108 | 0.457 | |
| | $\theta_5$ | 0.646 | 0.469 | | 0.442 | 0.472 | |
| | $\theta_6$ | 2.162 | 0.566 | | 2.285 | 0.595 | |
| *Fixed effect* | $\beta(TTA_{vis})$ | −0.870* | 0.071 | < 0.001 | −0.738* | 0.062 | < 0.001 |
| *Random effects* | subject | 4.755 | 2.181 | | 4.006 | 2.002 | |

*Note:* For random effects, *Estimate* corresponds to the estimate of the random effect variance. The star (*) represents the fixed effects that were statistically significant ($p < 0.05$). SD stands for standard deviation.

**Table 5**
Cumulative link mixed model for the simulator (including the surprise trial).

| Variables | | Estimate | SD | p-value |
|---|---|---|---|---|
| *Cut-points* | $\theta_1$ | −6.310 | 0.516 | |
| | $\theta_2$ | −4.303 | 0.468 | |
| | $\theta_3$ | −2.600 | 0.438 | |
| | $\theta_4$ | −1.215 | 0.427 | |
| | $\theta_5$ | −0.025 | 0.434 | |
| | $\theta_6$ | 1.284 | 0.475 | |
| *Fixed effects* | $\beta(TTA_{vis})$ | −0.954* | 0.068 | < 0.001 |
| *Random effect* | subject | 4.159 | 2.039 | |

*Note:* For the random effects, E(var.) is the estimate of the variance and E(std.) the estimate of its corresponding standard deviation. The star (*) represents the effects that were statistically significant ($p < 0.05$).

distributed participants effect (Y-axis) and $TTA_{vis}$ (X-axis).

For the three fitted CLMMs, the lower the $TTA_{vis}$, the more likely a high discomfort score; for the range of 3.5–7.0 s, the probabilities of getting discomfort scores of 1, 6, or 7 are similar. For the other scores, it is more likely that higher scores would be chosen in TT than in SIM or SIMST for a given value of $TTA_{vis}$. The CLMM fit for SIMST, which (unlike SIM) includes the surprise trials, is in line with the fit for SIM.

### 3.3. Estimation of prediction accuracy of the cumulative link model with mixed effects

The prediction accuracy of the CLMMs in Eqs. (5) and (6) was compared. The estimates of the prediction accuracy for each model and for each dataset are plotted in Fig. 6. The graph shows that the prediction accuracies seem to be similar, independent of the model or the dataset. Additionally, as one can expect, the more trials used for the fit, the higher the overall accuracy. The highest estimates of the overall accuracy were just below 50 %. It should be noted that the two models were similar in terms of accuracy, although the model CLMM($V_{bicycle}$, $V_{car}$, $Lat_{arr}$) included three predictors while CLMM($TTA_{vis}$) had only one. Finally, it can also be noted that the presence of the surprise trials did not seem to improve the model accuracy; however, the results presented below highlight the advantages of including them.

The confusion matrices obtained at the last point of the cross-validation process are presented in Fig. 7; the six confusion matrices correspond to the right endpoint of the six average curves of Fig. 6. As indicated by Fig. 6, the correct predictions were not the most frequent; none of the diagonals are a perfect diagonal with the lightest colour, which would be the result if the overall accuracy were higher. The light-coloured cells are located higher above the diagonal as the observed score increases. That is, for a higher observed score the models are more likely to predict a lower discomfort score. Comparing the confusion matrices for the three datasets suggests that the models using TT follow the diagonal better than the others. For a given observed score, this means that the models from TT were more likely to predict a score just below the observed score by one increment. The models from SIM and SIMST seem more likely to give a score below or equal to 4. Nonetheless, it has to be noted that the surprise trials (i.e. comparing SIMST to SIM), improved the accuracy of CLMM($TTA_{vis}$) at higher observed discomfort scores (see Fig. 7).

Finally, the overall accuracy for each confusion matrices (Fig. 7) when a difference of one unit between the observed and the predicted scores is considered as correct prediction were reported on Table 6.

## 4. Discussions

Two CLMMs were presented, one including three controlled variables ($V_{bicycle}$, $V_{car}$, and $Lat_{arr}$) and the other including only one variable ($TTA_{vis}$). Remarkably, the models were comparable for the datasets SIM, SIMST, and TT: the CLMM fits were similar in terms of their fixed effect estimates as well as their random effect estimates. In addition, the variability between participants in rating discomfort (see Fig. 4) was similar for the three datasets, which suggests that the two participant populations behaved similarly across experiments. In other words, the use of a fixed-base simulator—an inexpensive setup compared to a test-track setup— may be suitable to analyse driver discomfort in similar situations.

The model including the controlled variables showed that when the speeds increased, or when $Lat_{arr}$ decreased towards zero, participants were likely to report higher discomfort scores. This observation was made independently of the experimental setup and is explained by higher speeds and $Lat_{arr}$ close to zero implying a more critical situation. The second model, based only on $TTA_{vis}$, showed that the more critical the situation was (i.e. lower values of $TTA_{vis}$), the more likely drivers reported high discomfort (as hypothesised in the introduction). $TTA_{vis}$ and the three controlled variables $V_{bicycle}$, $V_{car}$, and $Lat_{arr}$ are related via a non-linear relationship; hence, the two studied CLMMs were expected to give similar results.

These models were designed to predict individual discomfort scores; however, their overall accuracy is roughly between 40 % and 50 % when looking at the number of exact predictions. It was shown that when increasing the tolerance of the prediction (i.e. considering a predicted score that falls within a -1/+1 range of the observed score as correct), the overall accuracy was around 80 %. Therefore, most of the time, the models predict a discomfort score that is of the order of magnitude of the one experienced by drivers, enabling potential active safety systems and automated driving systems algorithms to estimate at what level drivers' discomfort is. Noteworthy, the confusion matrices (Fig. 7) showed that the models were more accurate at lower scores than at higher scores, mostly because of the small number of trials with high scores compared to the ones with low scores. Furthermore, the results showed that CLMM($TTA_{vis}$) may be more appropriate than CLMM($V_{bicycle}$, $V_{car}$, $Lat_{arr}$) as a discomfort prediction algorithm in active safety systems or automated driving systems, because the former is

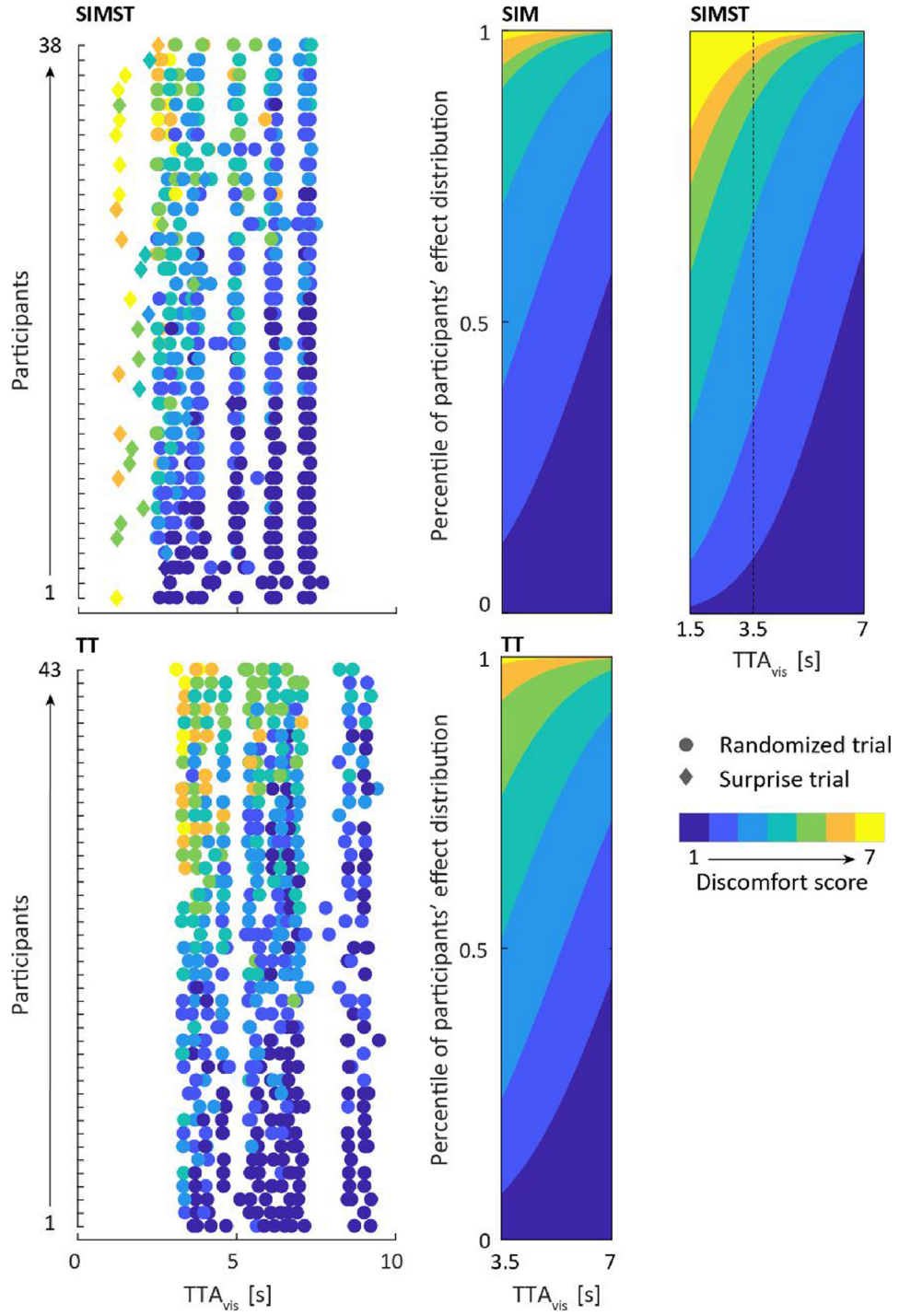


**Fig. 5.** Left-hand side: scatter plots show the distribution of discomfort scores per participant versus $TTA_{vis}$. Right-hand side: discomfort score with highest probability according to the fitted cumulative link mixed models against $TTA_{vis}$ and the percentile of participants' random effect. Top: SIM and SIMST, bottom: TT.

based on only one variable, necessitating fewer sensors. Finally, because the models are driver-dependent, an active safety system or automated driving system implementing it would have to be driver-adaptive and learn drivers' feeling of discomfort over time.

The results of CLMM($TTA_{vis}$) suggest that the discomfort in this scenario might be mainly driven by visual cues rather than deceleration cues. This is quite significant when it comes to automated driving systems, because it is likely that driver-passengers in a self-driving car will feel more discomfort than when driving themselves. Therefore, it is suggested that automated driving systems process visual information to avoid entering situations where drivers would feel discomfort. A previous paper (Boda et al., 2018) showed that drivers' braking reactions were driven by the same visual cue-based metric used by the model ($TTA_{vis}$). The relationship between feelings of discomfort and braking reaction has been suggested in the literature (Ljung Aust and Engström, 2010); if the discomfort is high it is quite likely that drivers will react by braking or steering, acting as fast as the situation requires it. Therefore, it is suggested that automated driving systems not brake later than drivers would normally brake themselves, and that they try to avoid situations where drivers would normally feel high discomfort. The latter suggestion has notable implications for driver acceptance.

In addition to providing recommendations for automated driving

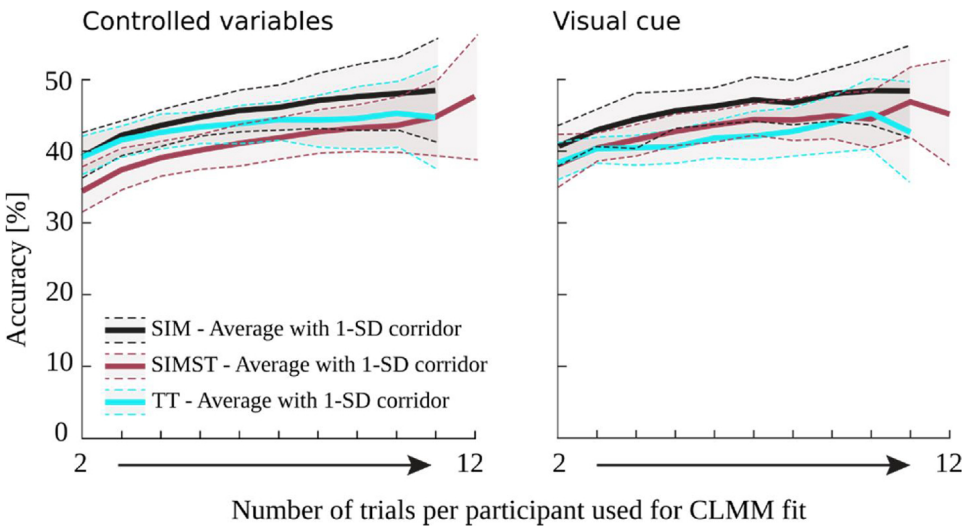


**Fig. 6.** Estimates of prediction accuracy versus the number of trials per participant used for fitting the CLMMs, with controlled variables as predictors (left) and $TTA_{vis}$ as predictor (right). The estimates of the accuracy together with their respective one-standard-deviation (1-SD) corridor are plotted for each dataset (SIM, SIMST, and TT).

system acceptance, these results could also apply to improve the acceptance of active safety systems such as FCW. The decision algorithms used to trigger warnings could benefit from a model such as CLMM ($TTA_{vis}$) (Ljung Aust and Dombrovskis, 2013). Depending on the time-to-arrival and the driver, the collision warning could be advanced to avoid warning the driver too late (creating feelings of great discomfort, incompatible with the driver's feeling of safety) or delayed to avoid a warning that is too early (creating feelings of annoyance at the system,

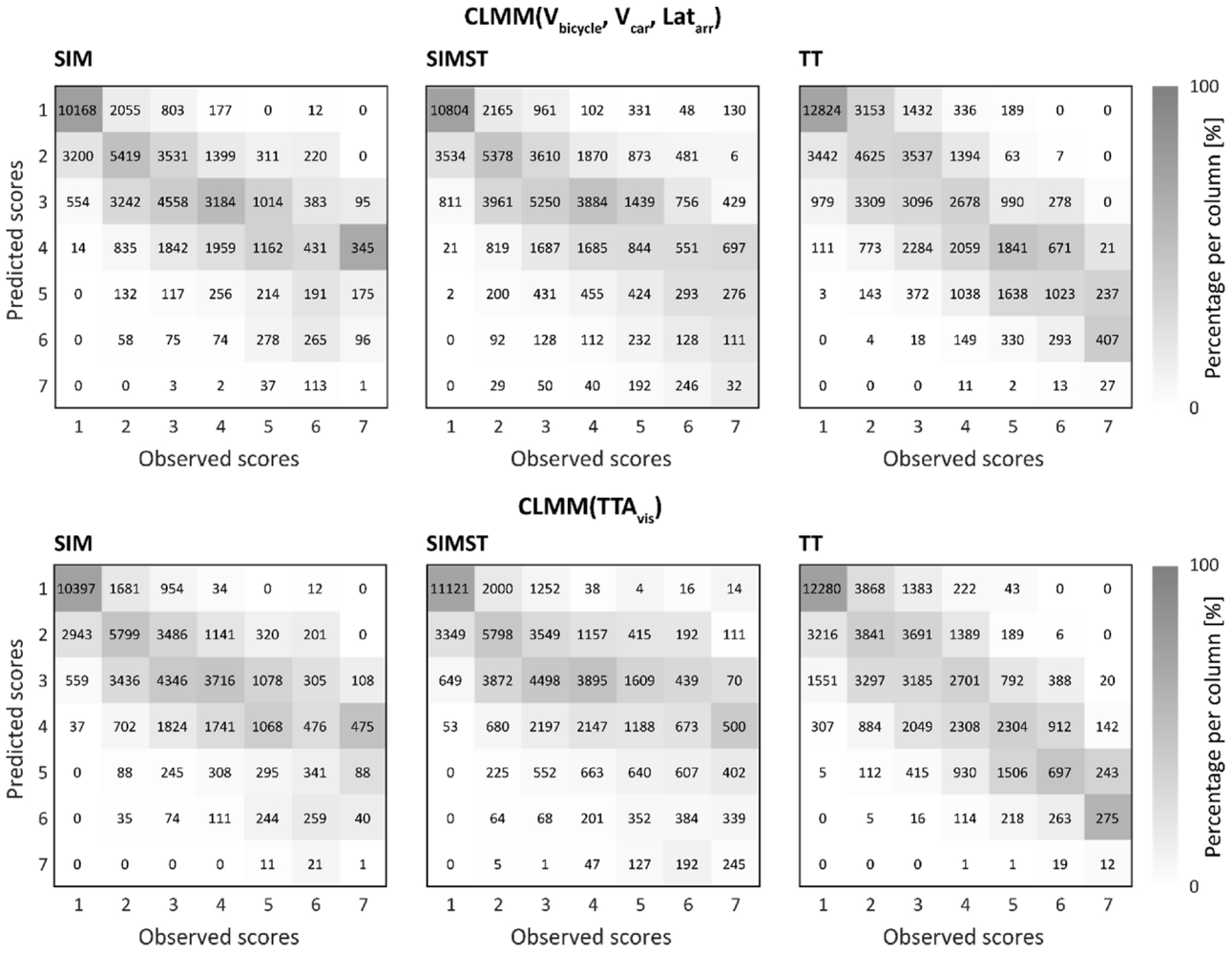


**Fig. 7.** Confusion matrices for CLMM($V_{bicycle}$, $V_{car}$, $Lat_{arr}$) (top row) and CLMM($TTA_{vis}$) (bottom row) for each dataset (SIM, SIMST, and TT). The matrices are the result of the predictions made when fitting the models with 11 trials per participant for SIM and TT and 12 for SIMST. The trials used for the fit were randomly drawn from each of the 200 Monte Carlo iterations. A greyscale represents the frequency of occurrence for each pair (predicted score, observed score); the lighter the colour, the more frequent the pair's occurrence.

**Table 6**
Accuracies when a tolerance of -1/+1 score is included for CLMM($V_{bicycle}$, $V_{car}$, $Lat_{arr}$) and CLMM($TTA_{vis}$).

| | SIM | SIMST | TT |
|---|---|---|---|
| CLMM($V_{bicycle}$, $V_{car}$, $Lat_{arr}$) | 85 % | 79 % | 85 % |
| CLMM($TTA_{vis}$) | 86 % | 83 % | 84 % |

because discomfort is still minimal). However, autonomous emergency braking systems that are activated when the situations become too critical would not benefit from delaying or advancing their intervention—because such systems are already designed to intervene only in critical situations, when the driver input is not sufficient to avoid a crash.

The following paragraph demonstrates how the discomfort model can be applied to improve active safety systems decision-making algorithms and which impact it has on the design of active safety system assessment programs such as the Euro NCAP. The experimental protocol in the present paper was derived from a scenario that has been added to the 2018 Euro NCAP evaluation protocol (Euro NCAP, 2018). In this scenario, only the performance of AEB is evaluated. The following specifications are used in the scenario: a constant bicycle speed of 15 km/h (the bicycle appears from the near side), car speed evaluated from 20 km/h to 60 km/h in 5 km/h increments, the bicycle and the car are controlled to achieve a 50 %-overlap collision if the car maintains its initial speed, and the bicycle starts to be visible approximately 4 s before the car reaches the collision point (i.e. $TTA_{vis}$ = 4.0 s). To achieve the maximum score, the AEB in the tested car should avoid collisions with the bicycle for car speeds up to 40 km/h, and the system should reduce the collision speed by 20 km/h when the car's speed (before activation) is 40 km/h–60 km/h (Euro NCAP, 2018). Because the AEB are designed to intervene at the last moment, the use of the discomfort model presented in the present study is limited. However, for a FCW (activation times from TTA = 1.07 s for a car speed of 20 km/h to TTA = 1.97 s for 60 km/h, see Appendix A), the use of the discomfort model would be possible and relevant. Assuming that the warning issued by the FCW would make the driver perceives the cyclist, the value of 1.97 s TTA corresponds to a low-critical situation in which around 50 % of drivers experienced a discomfort lower than 4 (Fig. 5). This means that most drivers in this situation would prefer a delayed warning (a shorter TTA). This finding refines the earlier recommendation for FCW activation at TTA between 1.8 s and 2.6 s based on observed brake onset (Boda et al., 2018). With this refinement, we believe using FCW in cyclist crossing situations is feasible and should therefore be considered by Euro NCAP.

In these experiments, participants were asked to execute a single task: driving through an intersection. When the cyclist appeared, the participants immediately saw it. The models presented here assume drivers to be attentive. Future work should investigate the effect of cognitive load and glance behaviour on discomfort. Furthermore, the discomfort scores given by drivers were most likely generated by the criticality of the trials. The discomfort model does not consider any other type of discomfort—caused by, for example, unexpected decelerations (car brakes faster than expected, or collides with an obstacle or another road user) or bad vehicle ergonomics. Also, the results suggest that discomfort is related to the moment when the bicycle appears (i.e. visual cues); they do not elucidate the extent to which discomfort may be induced by the predicted required deceleration, or by human instinct. Future investigations should compare the discomfort felt by experienced drivers to that felt by completely inexperienced drivers, to determine what role experience plays in discomfort levels (analogous to the experiment carried out by Benderius (2014), comparing children with adults driving in a driving simulator).

## 5. Conclusions

Visual cues from a fixed-base simulator and a combination of visual and deceleration cues from a test track resulted in similar levels of discomfort in drivers approaching an intersection while a cyclist was crossing their path. This result supports the ecological validity of fixed-base simulators as a means to model driver discomfort for the design of active safety intervention.

In both the test track and simulator experiments, participants' discomfort seemed to depend on the time left to reach the intersection at the moment in which the cyclist appeared. Although a combination of bicyclist speed, car speed, and lateral distance may also be used to explain discomfort, it is more likely that the timing of the cyclist's appearance is indeed the most important factor for the feeling of discomfort.

This study suggests that the activation threshold within active safety systems—including automated driving systems—should be adaptive and include perceived discomfort. In other words, a discomfort model should be included in the threat assessment and decision making of systems like FCW. The discomfort model would support the traditional kinematics models by adapting the timing of the safety system's activation to the level of discomfort that may be experienced by drivers under normal circumstances (e.g. when the driver is attentive). Thus, such a model would favour earlier interventions when acceptance may be higher (due to greater discomfort) and avoid earlier interventions when the situation is perceived as less critical and driver discomfort is expected to be lower.

The results presented in this paper apply to a specific intersection scenario, in which a cyclist crosses the path of an attentive driver approaching an intersection. Generalization to other scenarios (including, for example, other road users or impaired drivers) requires further work.

## Acknowledgements

The authors would like to thank Carol Flannagan for her support with cumulative link models with mixed effects. Markus Pastuhoff, Sonny Muhoray, Peter Andersson, and Börje Jansson are as well thanked for setting up the test-track experiment and assisting with data collection. Additionally, the authors acknowledge Kristina Mayberry for language revisions. This study was part of the project Drivers in Interaction with Vulnerable Road Users funded by Toyota Motor Europe (Belgium) and Autoliv (Sweden). This project was performed at SAFER the Vehicle and Traffic Safety Center at Chalmers.

## Appendix A

For demonstration purposes, activation times of an AEB and a FCW were evaluated in the Euro NCAP CBNA-50 scenario. The implemented algorithms were modelled according to Section III-C in the paper by Brännström et al. (2010). Their model was designed to avoid imminent collisions, rather than merely reducing collision speed by 20 km/h for higher car speeds than 40 km/h (as the Euro NCAP rating requires). Some simplifications were made; only the avoidance manoeuvre by deceleration was implemented, with an infinite jerk and a maximum deceleration threshold of 1.0 g for AEB and 0.5 g for FCW. The AEB deceleration threshold was based on the limits of vehicle dynamics, while the FCW threshold was based on a deceleration level considered comfortable for drivers (Brännström et al., 2014). In the Euro NCAP scenario, the modelled AEB—activated at the last moment—would be triggered at around TTA = 0.28 s for a car speed of 20 km/h and at TTA = 0.84 s for 60 km/h. The modelled FCW would be activated at TTA = 1.07 s for a car speed of 20 km/h and at TTA = 1.97 s for 60 km/h. These TTA values incorporate an average driver's reaction time of 0.5 s in critical situations (Boda et al., 2018).

## Appendix B. Supplementary data

Supplementary material related to this article can be found, in the online version, at doi:https://doi.org/10.1016/j.aap.2020.105550.

## References


Adell, E., Varhelyi, A., Nilsson, L., 2014. The definition of acceptance and acceptability. Driver Acceptance of New Technology: Theory, Measurement and Optimisation. Farnham, UK, Ashgate Publishing, pp. 11–21.

Agresti, A., 2013. Categorical Data Analysis. Wiley, Hoboken, NJ.

Benderius, O., 2014. Modelling Driver Steering and Neuromuscular Behaviour. Ph.D., Chalmers University of Technology.

Boda, C.-N., Dozza, M., Bohman, K., Thalya, P., Larsson, A., Lubbe, N., 2018. Modelling how drivers respond to a bicyclist crossing their path at an intersection: How do test track and driving simulator compare? Accid. Anal. Prev. 111, 238–250.

Börjesson, M., Eliasson, J., 2012. The value of time and external benefits in bicycle appraisal. Transp. Res. Part A Policy Pract. 46 (4), 673–683.

Brännström, M., Coelingh, E., Sjöberg, J., 2010. Model-based threat assessment for avoiding arbitrary vehicle collisions." Intelligent Transportation Systems. IEEE Trans. 11 (3), 658–669.

Brännström, M., Sandblom, F., Hammarstrand, L., 2013. A probabilistic framework for decision-making in collision avoidance systems." intelligent transportation systems. IEEE Transactions on 14 (2), 637–648.

Brännström, M., Coelingh, E., Sjöberg, J., 2014. Decision-making on when to brake and when to steer to avoid a collision. ." International Journal of Vehicle Safety 7 (1), 87–106.

Christensen, R.H.B., 2015. ordinal—Regression Models for Ordinal Data.

Colby, E., Bair, E., 2013. Cross-validation for nonlinear mixed effects models. J. Pharmacokinet. Pharmacodyn. 40 (2), 243–252.

Dagan, E., Mano, O., Stein, G.P., Shashua, A., 2004. Forward collision warning with a single camera. . IEEE Intelligent Vehicles Symposium 2004.

Engström, J., 2011. Understanding Attention Selection in Driving: From Limited Capacity to Adaptive Behaviour. Chalmers University of Technology.

Euro NCAP, 2018. Euro NCAP Assessment Protocol AEB VRU Test Protocol v2.0.2. Assessment Protocol. Euro NCAP.

European Commission, 2017. Annual Accident Report European Commission. Directorate General for Transport.

Hayashi, H., Inomata, R., Fujishiro, R., Ouchi, Y., Suzuki, K., Nanami, T., 2013. Development of pre-crash safety system with pedestrian collision avoidance assist. Proceedings of the 23rd International Technical Conference on the Enhanced Safety of Vehicles (ESV) 13.

Jamson, A.H., Lai, F.C.H., Carsten, O.M.J., 2008. Potential benefits of an adaptive forward collision warning system. Transp. Res. Part C Emerg. Technol. 16 (4), 471–484.

Kiefer, R.J., 2000. Developing a forward collision warning system timing and interface approach by placing drivers in realistic rear-end crash situations. In: Proceedings of the Human Factors and Ergonomics Society Annual Meeting. SAGE Publications.

Ljung Aust, M., Dombrovskis, S., 2013. Understanding and improving driver compliance with safety system feedback. In: Proceedings of the 23rd International Technical Conference on the Enhanced Safety of Vehicles. Seoul, Republic of Korea.

Ljung Aust, M., Engström, J., 2010. A conceptual framework for requirement specification and evaluation of active safety functions. Theor. Issues Ergon. Sci. 12 (1), 44–65.

Ljung Aust, M., Jakobsson, L., Lindman, M., Coelingh, E., 2015. Collision Avoidance Systems - Advancements and Efficiency. SAE International.

Lubbe, N., Rosén, E., 2014. Pedestrian crossing situations: quantification of comfort boundaries to guide intervention timing. Accid. Anal. Prev. 71 (0), 261–266.

Markkula, G., Engström, J., Lodin, J., Bärgman, J., Victor, T., 2016. A farewell to brake reaction times? Kinematics-dependent brake response in naturalistic rear-end emergencies. Accid. Anal. Prev. 95, 209–226 Part A.

Martens, K., 2007. Promoting bike-and-ride: the Dutch experience. Transp. Res. Part A Policy Pract. 41 (4), 326–338.

Prati, G., Marín Puchades, V., De Angelis, M., Fraboni, F., Pietrantoni, L., 2017. Factors contributing to bicycle–motorised vehicle collisions: a systematic literature review. Transp. Rev. 1–25.

Pucher, J., Buehler, R., Seinen, M., 2011. Bicycling renaissance in North America? An update and re-appraisal of cycling trends and policies. Transp. Res. Part A Policy Pract. 45 (6), 451–475.

Scheepers, C.E., Wendel-Vos, G.C.W., den Broeder, J.M., van Kempen, E.E.M.M., van Wesemael, P.J.V., Schuit, A.J., 2014. Shifting from car to active transport: a systematic review of the effectiveness of interventions. Transp. Res. Part A Policy Pract. 70 (Supplement C), 264–280.

Schepers, P., Kroeze, P.A., Sweers, W., Wüst, J.C., 2011. Road factors and bicycle–motor vehicle crashes at unsignalized priority intersections. Accid. Anal. Prev. 43 (3), 853–861.

Schepers, P., Stipdonk, H., Methorst, R., Olivier, J., 2016. Bicycle fatalities: trends in crashes with and without motor vehicles in the Netherlands. Transp. Res. Part F Traffic Psychol. Behav.

Silvano, A.P., Koutsopoulos, H.N., Ma, X., 2016. Analysis of vehicle-bicycle interactions at unsignalized crossings: a probabilistic approach and application. Accid. Anal. Prev. 97, 38–48.

Story, M., Congalton, R., 1986. Accuracy assessment: a user's perspective. Photogramm. Eng. Remote Sensing 52 (3), 397–399.

Summala, H., 2007. Towards understanding motivational and emotional factors in driver behaviour: comfort through satisficing. Modelling Driver Behaviour in Automotive Environments. Springer, pp. 189–207.

Tsuchida, J., Tokoro, S., Fujinami, H., Usami, M., 2007. The advanced sensor fusion algorithm for pre-crash safety system. SAE International.